Realtime MRI detection of systemically injected iron-labeled mesenchymal stem cells in the infarcted rat myocardium

Bum-Kee Hong

Department of Medical Science
The Graduate School, Yonsei University

Realtime MRI detection of systemically injected iron-labeled mesenchymal stem cells in the infarcted rat myocardium

Directed by Professor **Seung Yun Cho**

The Doctoral Dissertation
submitted to the Department of Medical Science,
the Graduate School of Yonsei University
in partial fulfillment of the requirements for the degree of Doctor of Philosophy of Medical Science

Bum-Kee Hong

December 4, 2005

This certifies that the Doctoral Dissertation of Bum-Kee Hong is approved.

Thesis Supervisor: **Seung-Yun Cho**

Thesis Committee Member#1: **Sang-Ho Cho**

Thesis Committee Member#2: **Byung Chul Chang**

Thesis Committee Member#3: **Yangsoo Jang**

Thesis Committee Member#4: **Hyun Cheol Chung**

The Graduate School
Yonsei University

December 4, 2005

ACKNOWLEDGEMENTS

First, I would like to express my gratitude to Dr. Seung-Yun Cho for being an outstanding advisor and excellent professor. His constant encouragement, support, and invaluable suggestions made this work successful. He has been everything that one could want in an advisor. I am also deeply indebted to my committee members Dr. Sang-Ho Cho, Dr. Byung-Chul Chang, Dr. Yanhsoo Jang, and Dr. Hyun Cheol Chung for their time and effort in reviewing this work.

My sincere thanks go to Dr. Cynthia E. Dunbar in National Institute of Health for making me work there for two years as well as helping me fulfill this research. I am deeply indebted to Jonathan Sorger, who had been a research fellow in National Institute of Health, for making me a better animal surgeon as well as helping me overcome many technical problems. I am also grateful to Mikko O. Laukkanen and Calmels Boris for their help and valuable advices, and for being great friends throughout my stay at institute.

Last, but not least, I am deeply and forever indebted to my parents for their love, support and encouragement throughout my entire life. I would like to express my deepest gratitude for the constant support, understanding, and love that I have received from my wife Eun-Young, son Ju-Wan, and daughter Yeon-Jung.

TABLE OF CONTENTS

LIST OF FIGURES

ABSTRACT

Realtime MRI detection of systemically injected iron-labeled mesenchymal stem cells in the infarcted rat myocardium

Bum-Kee Hong

Department of Medical Science
The Graduate School, Yonsei University

(Directed by Professor **Seung Yun Cho**)

Cell therapy using adult pluripotent stem cells is limited by the inability to track in vivo engraftment and the fate of transplanted cells. Recent evidence has demonstrated the homing ability of mesenchymal stem cells to bone marrow following systemic infusion. Homing of stem and progenitor cells to myocardial injury is one potential mechanism that may permit a non-invasive approach to cardiovascular cell therapy. Cellular based contrast agents were initially used to monitor T cell trafficking in inflammation and, more recently, have been used to track stem cells for neurological applications. Stem cell migration has been demonstrated in healthy and damaged brain tissue of rodents and tracked using gadolinium based agents. Recent evidence has demonstrated the feasibility of iron labeling of stem and progenitor cells without affecting differentiation and proliferation and for monitoring cell engraftment following direct myocardial injection.

In an attempt to assess the homing of systemically injected mesenchymal stem cells to infarcted myocardium, this study was initiated with a series of experiments aimed at tracking of these cells which had been labeled with iron oxide microparticles, followed by assessing whether these cells can express cardiomyocyte-specific proteins and contribute the functional competence.

Myocardial infarction was induced in sixteen August Copenhagen Irish (ACI) rats by

surgical occlusion of the left coronary artery followed by reperfusion and intravenous administration of either allogeneic iron-fluorescence-particle (IFP)-labeled mesenchymal stem cells derived from ACI rats (n=9) or free IFP (n=9). Serial cardiac MRI exams were performed at fifth day, sixth week, third month, and sixth month. The presence of IFP-labeled stem cells was confirmed using confocal microscopy and immunohistochemistry for desmin and connexin-43, the markers of cardiomyogenic differentiation. The total number of cells was counted in both infarcted and non-infarcted tissue and compared to the total number of engrafted IFP-labeled cells.

IFP-labeled MSCs were detected from as early as 5 days after injection up to 6 months in infarcted region (the peak at sixth week). IFP-labeled MSCs preferentially home to the site of myocardial injury, with a significantly higher labeled-cell to total cell ratio within the infarct zone compared to normal myocardium (0.62 vs 0.16, $p< 0.001$). At sixth week the engrafted MSCs expressed sarcomeric and gap junction proteins (desmin and connexin-43), which exhibited the maturation of their structural patterns at third month. In left ventricular ejection fraction, even though there was no statistical significance, there was a trend for the MSCs-treated animals to exhibit greater recovery of systolic function than that of the control.

This study demonstrates the feasibility of using MRI to track the homing and preferential engraftment of allogeneic mesenchymal stem cells as they traffic to the sites of tissue injury and seem to differentiate into cells with cardiomyocyte phenotype.

Key Words: mesenchymal stem cell, iron-fluorescence particle, myocardial infarction, magnetic resonance imaging, homing, differentiation, desmin, connexin-43

Realtime MRI detection of systemically injected iron-labeled mesenchymal stem cells in the infarcted rat myocardium

Bum-Kee Hong

Department of Medical Science
The Graduate School, Yonsei University

(Directed by Professor **Seung Yun Cho**)

I. INTRODUCTION

Recent reports of the discovery of human pluripotent stem cells that can differentiate into any cell type found in the body have led to a wealth of research and controversy in the field of tissue repair[1,2]. While embryonic stem cells have received most of attention as a source of tissue regeneration, adult stem cells, which can be found in neural, skeletal and adipose tissues in addition to bone marrow have been shown to exhibit a degree of pluripotency[3-10]. It is possible that adult stem cells may offer therapeutic benefits similar to those of embryonic cells.

The use of bone marrow-derived stem cells allows autologous transplants, which reduces the possibility of immune system rejection. Bone marrow derived adult stem cells have been shown to differentiate into neural astrocytes and cardiomyocytes[11,12]. Orlic, et al. has shown that mobilized bone marrow cells, when injected directly adjacent to an infarcted region of murine myocardium, differentiate into myocytes, vascular endothelium and smooth muscle cells[13]. Mice receiving the cells exhibited significantly higher ejection fractions than those not receiving the transplant. In another study, left ventricular wall thickness was increased and collagen deposition decreased[14].

While the Ferrari study showed that bone marrow cells could differentiate into myoblasts,

it did not indicate the type of stem cell population responsible for the regenerated muscle fibers. Hematopoetic (HSC) and mesenchymal stem cells (MSCs) both reside in the bone marrow. HSC differentiate into various types of blood cells while MSCs become adipocytes, chondrocytes, osteoblasts and other cells that support the stroma. MSCs make up an extremely small percentage of bone marrow cells (0.001% to 0.01%), and have been located in adipose tissue, muscle, skin in addition to other locations of the body[15,16]. Due to the difficulty in identifying MSCs in vivo it has been challenging to precisely locate and quantify the MSC population but some studies indicate that the MSC population decreases with age[17]. While it was originally thought that tissue-specific stem cells did not exhibit the same amount of plasticity as embryonic stem cells, recent studies have demonstrated that marrow stromal cells can differentiate to form neural cells and cells with a cardiomyocyte phenotype[18,19].

Since they reside in the bone marrow, it is possible to obtain MSCs via normal aspiration. They can then be cultured for autologous transplantation, avoiding possible immune system complications. Data suggests that major and minor histocompatibility complexes affect cell transplantation effectiveness[20,21]. Autologous cell therapy would obviate the need for histocompatibility complex matching. MSCs are currently being used in clinical trials relating to osteogenesis imperfecta, lymphoma, myeloma and stroke[22-24]. While MSCs were discovered almost 40 years ago, the successful isolation and culture-expansion of a homogeneous batch of human MSCs has made research involving such cells much easier[25]. However, it has recently been reported that the late-passage growth rate of MSCs varies from donor to donor, with a loss of chondrogenic potential beyond passage five and decreased osteogenic potential beyond passage eight[26]. Most importantly, the loss of plasticity of these cells in culture was not detected by a change in phenotype. With their pluripotency, MSCs have great potential for the repair of tissue injured during myocardial infarction. Once localized to the area of injury, it is possible that MSCs can differentiate into cardiac myocytes and aid in the generation of new muscle to replace scarred tissue, affecting contractility. In doing so, MSCs may reduce the size of the 'at risk' region adjacent to the infarct or even enhance angiogenesis.

However, cell therapy using adult pluripotent stem cells is limited by the inability to track in vivo engraftment and the fate of transplanted cells. Recent evidence has

demonstrated the homing ability of mesenchymal stem cells to bone marrow following systemic infusion[27]. Therefore, in vivo non-invasive tracking approach could be a potential prerequisite to figure out the mechanisms of homing and differentiation of transplanted stem and progenitor cells. Cellular based contrast agents were initially used to monitor T cell trafficking in inflammation and, more recently, have been used to track stem cells for neurological applications[28-30]. Stem cell migration has been demonstrated in healthy and damaged brain tissue of rodents and tracked using gadolinium based agents[29,31-33]. Recent evidence has demonstrated the feasibility of iron labeling of stem and progenitor cells without affecting differentiation and proliferation and for monitoring cell engraftment following direct myocardial injection[34-37]. Therefore, in an attempt to assess the homing of systemically injected mesenchymal stem cells to infarcted myocardium, this study was initiated with a series of experiments aimed at tracking of these cells which had been labeled with iron oxide microparticles, followed by assessing whether these cells can express cardiomyocyte-specific proteins and contribute the functional competence.

II. MATERIALS AND METHODS

1. Cell expansion and labeling

Rat mesenchymal stem cells were derived from bone marrow aspirates from healthy adult AugustCopenhagen Irish (ACI) rats as previously described[15]. The cells were resuspended in mesenchymal stem cell growth medium (Poeitics, Biowhittaker, Walkersville, MD, U.S.A.) and seeded at concentrations of 1,000 cells/mm^2. After 3 days, non-adherent cells were removed and adherent colonies further expanded. Superparamagnetic fluorescent microspheres containing Flash Red or Dragon Green fluorochromes with an average diameter of 0.9m (Bangs Laboratories, Inc. IN, U.S.A.) were added to the cell culture medium for 18 hours prior to trypsinization (10/ml) as recently described[38].

An image of rat MSCs labeled with the iron fluorophore is shown in Figure 1. It was discovered that xylene destroys the fluorescent properties of the microspheres. The importance of this cannot be understated, as xylene is routinely used to remove paraffin from tissue in histologic processing. As a result, most of the tissues in the following experiments were snap-frozen in liquid nitrogen to preserve the antigenicity of the tissue and particle fluorescence, then sliced on a cryostat in preparation for histology and immunohistochemistry.

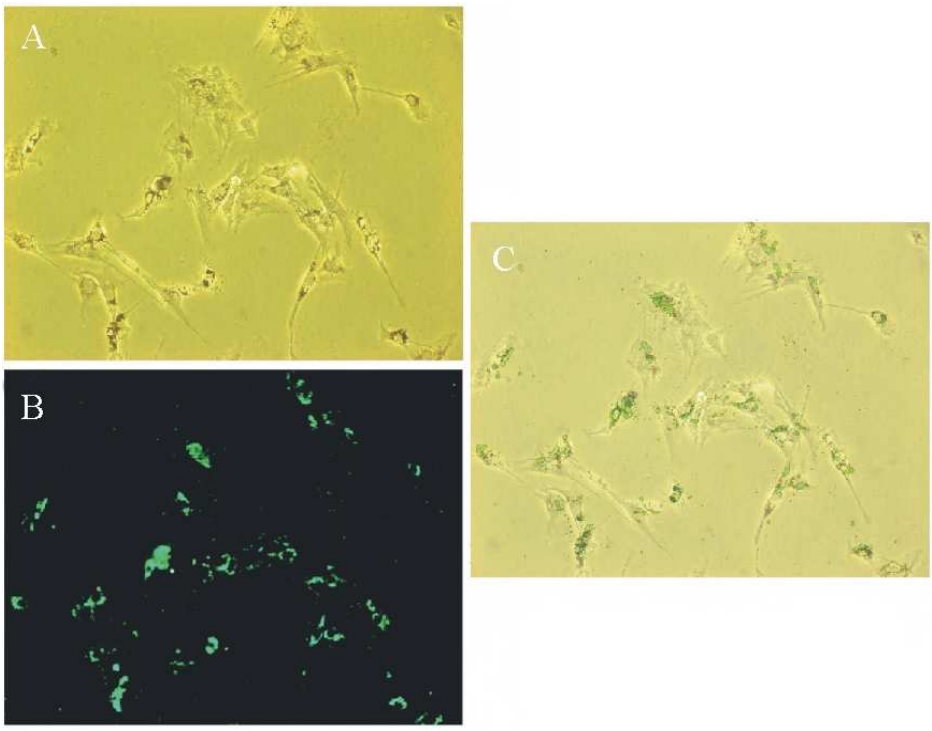

Figure 1. A light image of plated, labeled cells reveals iron particles within rat MSCs that allow tracking with MRI (**A**). The excitation of the particles by a fluorescent lamp illuminates their fluorescent properties, which allows their detection via histology (**B**). An overlay of the two photos illustrates the dual properties of the particles (**C**).

2. Animal Model

Anesthesia was induced using an induction chamber and maintained on 1～3% isoflurane, administered through intubation. The animal was placed on a heated water blanket and monitored via ECG/capnography.

Myocardial infarction was surgically induced in 18 male ACI rats as follows; After cutting and removing pericardial fat and accompanying pericardium with microscissor, key anatomical structures including left atrial appendage, the left ventricle and possibly the right ventricle were identified. At a level approximately upper 1/3 the length of anterior side of the heart from the apex, 7-0 suture was used to tie off a section perpendicular to the long axis of the heart (a piece of polyethylene tubing was inserted between the suture and myocardium prior to tightening the suture.). While the left coronary artery cannot be seen since it runs beneath the tissue, this caused a detectable area of ischemia in the left ventricle when tied. The occlusion of the left coronary artery was maintained for an hour, after which the tubing was removed and the suture cut to add reperfusion injury. During awakening rat after surgery, $8\text{-}10\times10^{6}$ iron-fluorescence particle (IFP)-labeled rat MSCs per kg of body weight were injected to rats (n=9) via the tail vein over 20 minutes in a volume of 1mlThe rate of infusion was limited to 0.05 ml/min due to the fact that MSCs lodge in the lungs after intravenous infusion. For control (n=9), we injected only free IFP without MSCs. When the rate of administration was increased beyond 0.05 ml/min, five rats developed pulmonary problems ranging from tachypnea (n=2) to death (n=3).

3. MRI parameters

A. *In vivo* imaging parameters

All *in vivo* studies were performed using either an Oxford Instruments (Oxford Magnet Technology, United Kingdom) 4.7T/40 cm or a Magnex (Magnex Scientific, United Kingdom) 7T/20 cm horizontal bore magnet using a Bruker Instruments Avance console, controlled by Paravision software (Bruker, Ettlingen, Germany). *In vivo* scans were performed using slice selective gradient echo imaging sequences with a flip angle of 20°, pixel size of 200×200×2,000 μm, a pulse repetition time of 26 ms and an echo

time of 2.6 ms with central k-space echos acquired first. Three 2 mm short axis slices and one long axis slice were acquired per animal at heart rates ranging from 300～400 beats per minute.

B. *Ex vivo* imaging parameters

Following euthanasia, *ex vivo* MRI scan was performed on an Oxford Instruments 7T/81 mm vertical bore magnet running Paravision. *Ex vivo* scan parameters included a 3D gradient echo imaging sequence with a flip angle of 30°, pixel size of 60×60 ×100 μm, a matrix size of 2,563, a pulse repetition time of 300 msec and an echo time of 2.6-3.1 msec.

4. Histological analysis

Sections were stained with Prussian Blue to confirm the presence of the intracellular iron particles. Immunohistochemistry was performed using an anti-desmin antibody (Dako, Carpinteria, CA, U.S.A., 1:100 dilution), anti-connexin 43 (Dako, Carpenteria, CA, U.S.A., 1:50 dilution), and anti-alpha actinin (Pharmingen, San Diego, CA, U.S.A., 1:100 dilution). Slides were coincubated with the antibody at 4℃ overnight before the application of a fluorescent secondary antibody.

5. Ejection Fraction Analysis

Using MRI data, an implementation of the modified Simpson's rule was used to compute left ventricular end-diastolic and end-systolic volumes, from which left ventricular ejection fraction was computed. Such a model uses short-axis images at the mitral valve and papillary muscle levels to compute the volumes of a stack comprised of a basal cylinder, a truncated cone, and an apical cone. The short-axis boundary areas of the left ventricle at mitral valve (Am) and papillary muscle levels were contoured off-line using Paravision software. The boundary between the endocardium and blood pool was traced, excluding the papillary muscles. The length of the left ventricular cavity was measured from the long axis view as the distance from the left ventricular apical endocardium to the midpoint of the mitral annulus. Volume (V) at end diastole and end systole was computed as: (Am)L/3 + (Am+Ap)L/6 + (Ap)L/9.

III. RESULTS

1. MRI Results

A. *In vivo* tracking of systemically infused MSCs

Once it was confirmed that MSCs preferentially migrated to the infarct and could be detected with ex vivo MRI, the same experiment was reproduced with *in vivo* scanning. Eight rats underwent the procedure with iron-labeled cells, undergoing cardiac MRI examinations at 24 hours, 48 hours, 72 hours and five days after surgery.

In general, tissue edema from the invasive surgical procedure prevented the acquisition of high quality images at 24 hours. A susceptibility induced contrast artifact attributed to the presence of MSCs was noted in 7/8 of the treated animals by fifth day. which is compared to the absence of dark signal in control heart (figure 2A).

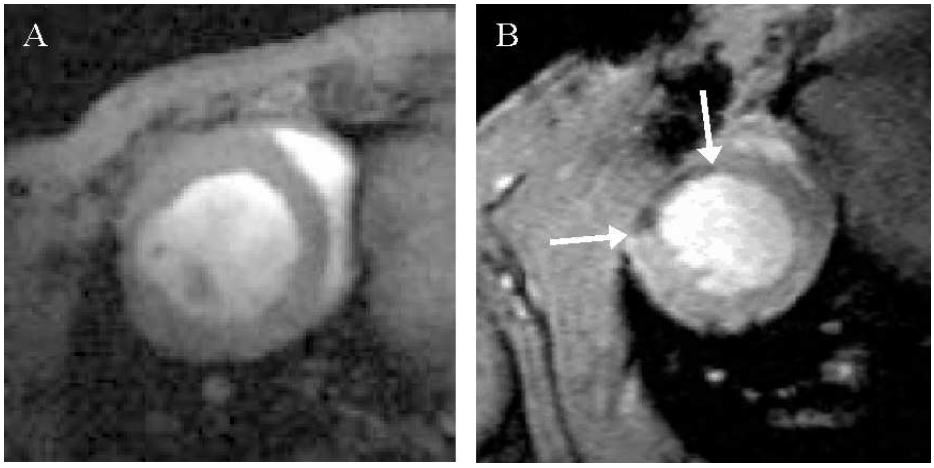

Figure 2. A short axis view of a rat heart five days after infarction in control rat (**A**) and in rat injected with iron-labeled mesenchymal stem cells (**B**). The anterior wall infarct (between the two arrows in B) is akinetic and has a signal intensity that is 33% lower than a healthy region of myocardium.

B. *Ex vivo* MRI results

Following euthanasia, MRI microscopy was performed on the rat hearts in order to more precisely determine the location of the cells. Three-dimensional data sets were acquired over a period of approximately 16 hours. Due to the amount of labor involved in performing histology and immunohistochemistry, scanning through the 3D data to locate tissue regions of interest improves the efficiency of tissue processing. An example of a high-resolution 3D data set is shown in figure 3 and 4.

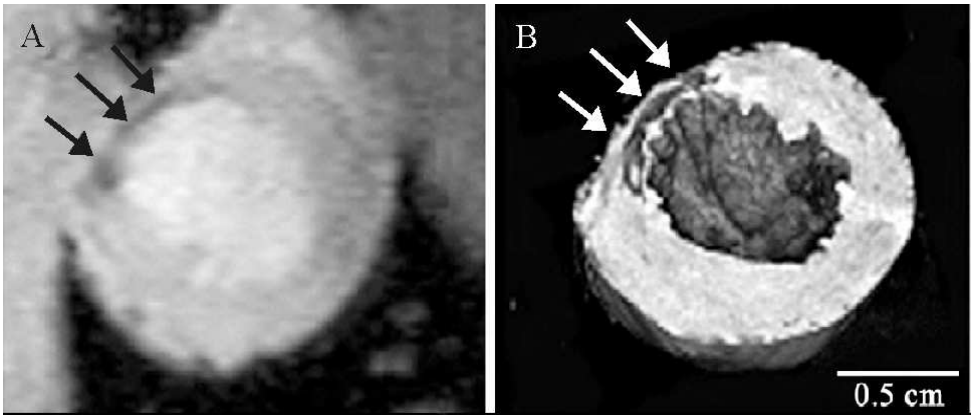

Figure 3. A comparison between the *in vivo* short axis image from figure 2B (**A**) and the ex vivo higher resolution three-dimensional data set of the same heart (**B**). Note the presence of the susceptibility artifact caused by the presence of the iron- labeled cells (arrows).

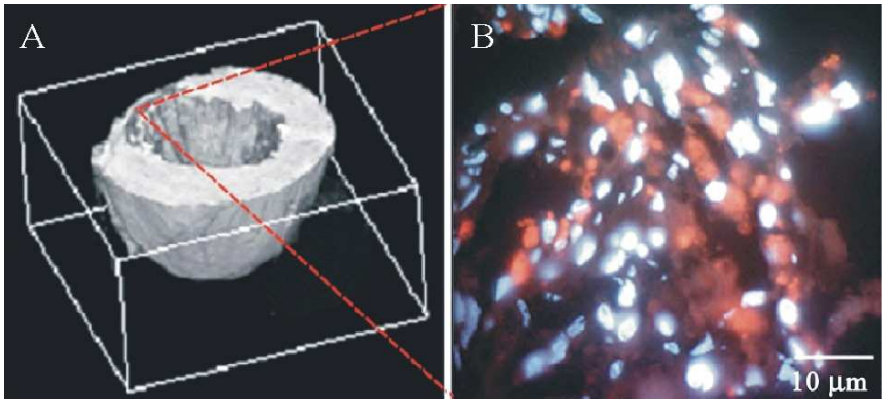

Figure 4. Three-dimensional data sets (**A**) can be used to guide tissue selection for histology. Instead of blindly searching for cells, the susceptibility artifact allows extraction of tissue containing the iron-laden cells. Cell nuclei are shown in blue, while fluorescently labeled iron particles are shown in red (**B**).

Eight rats were euthanized six weeks after surgery. Cells were detectable in the infarct zone in 7/8 animals, as shown in figure 5.

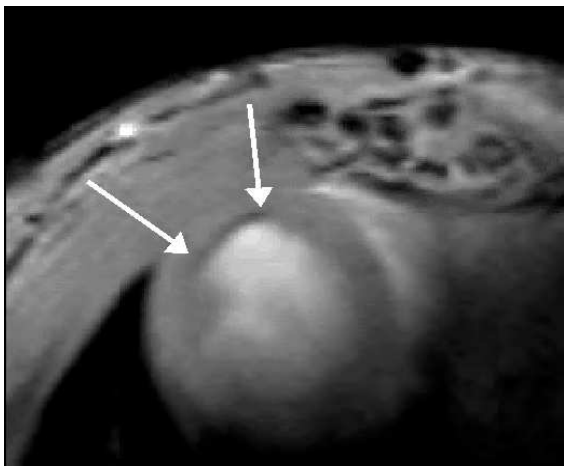

Figure 5. A short axis view of a rat heart six weeks after infarction and the administration of iron-labeled mesenchymal stem cells. The anterior wall infarct (between the two arrows) is visibly darker than regions of healthy myocardium. The susceptibility artifact is present in every time frame of the cine acquisition.

Using the 3D data sets to guide the histology, immunohistochemistry was performed on the hearts from these animals. Cells were detected by MRI and via histology in seven of the eight animals. The tail vein catheter became dislodged during one of the injections and it is possible that the bulk of the cells were injected in the subcutaneous region of the tail, accounting for the absence of cells in the heart in one of the animals.

2. Histological results

Histology was used to confirm the presence of cells in the infarct area. A Prussian Blue stain for iron is shown in figure 6. In such a stain, iron shows up in blue and normal tissue is shown in pink. A thin vein of blue cells runs through the infarct. A higher power view confirms the fact that the blue spots are cells with iron filling their cytoplasm.

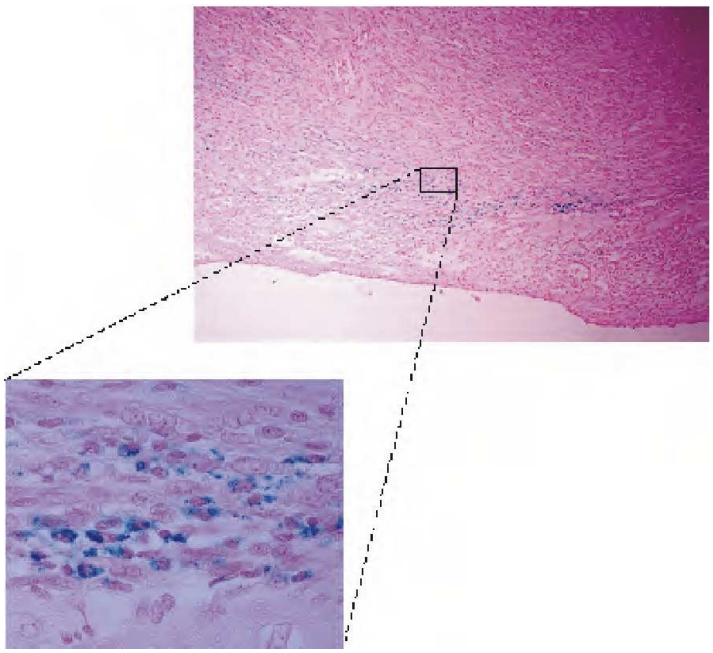

Figure 6. A Prussian Blue stained sample of one of the hearts five days after surgery and subsequent administration of MSCs. The presence of iron is indicated by the blue color and normal tissue shows up in pink. A thin vein of blue runs through the infarct. A higher power view confirms the presence of iron-laden cells.

In general, cells localized to the infarct. However, small numbers were also seen in slices more basal to the infarct; such cells were found clustered around the coronary arteries on the left side of the heart, as shown in figure 7 and were absent around the coronaries in the right side of the heart.

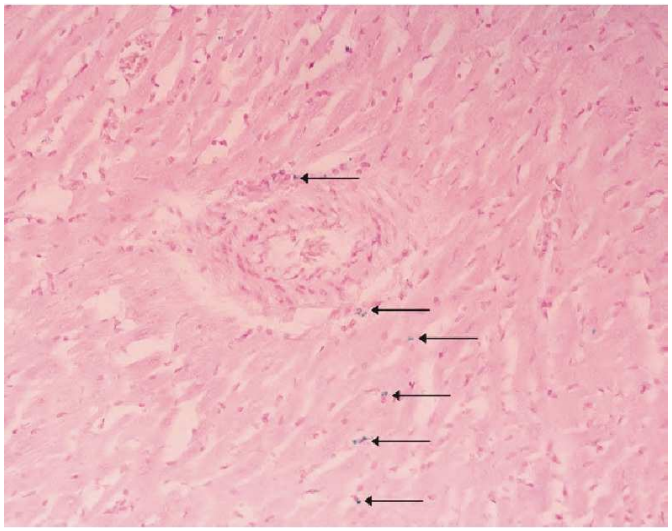

Figure 7. The presence of iron-laden cells localized around the left coronary artery in slices significantly basal to the infarction (arrows). Similar findings were not seen on the right side of the heart.

A. Early desmin expression

Cell nuclei were counterstained with DAPI and the relative engraftment of IFP-labeled cells compared in infarcted and normal myocardium (figure 8). The absolute number of IFP-labeled cells within the infarct zone was significantly increased compared to non-infarct zone (5,650±610/mm^2 vs. 720±290/mm^2, $p<0.001$). There was a significantly higher IFP-labeled cell to total cell ratio within the infarct zone compared to normal myocardium (0.62 vs 0.16, $p<0.001$).

At sixth week, large numbers of MSCs were found in the infarct zone, as shown in figure 9. The majority of iron-labeled cells (orange) are concentrated within the infarct zone. Figure 9B reveals IFP-labeled cells coexpressing desmin (green). However, such cells are devoid, for the most part, of striations typical of muscle tissue.

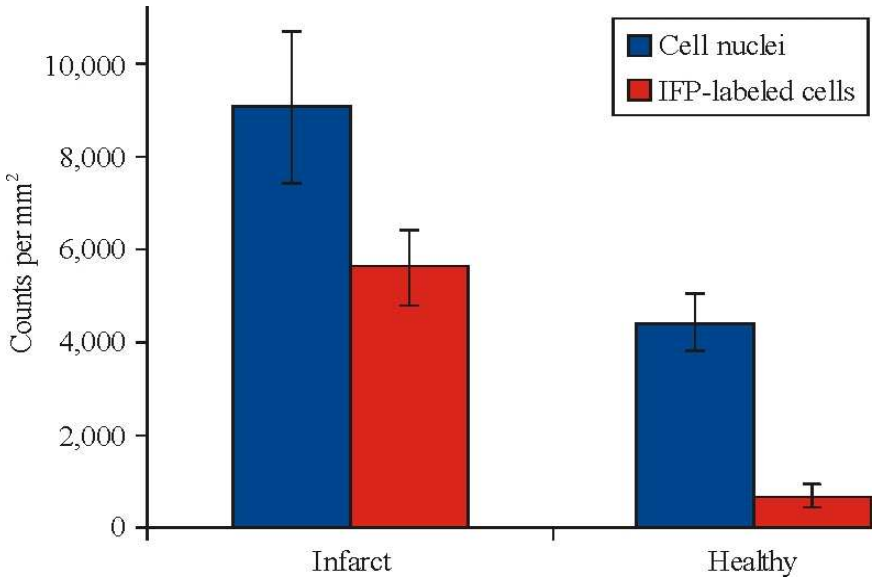

Figure 8. A comparison between the number of iron-labeled cells in infarct vs. non-infarct region six weeks after the procedure for eight animals. Significantly higher numbers of cells and cell nuclei are seen in the infarct region ($p<0.01$).

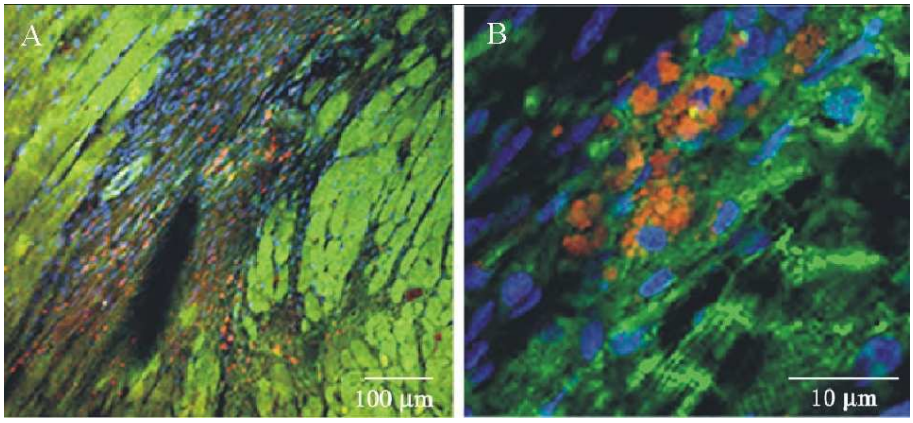

Figure 9. (**A**) Representative confocal micrograph at sixth week reveals IFP-labeled cells (orange) localized to the central infarct zone co-expressing desmin (green). Nuclei are counterstained with DAPI (blue). (**B**) High power view of the infarct zone showing healthy striated cells with adjacent IFP cells co-expressing desmin.

B. Early connexin-43 expression

IFP-labeled MSCs began to express connexin-43 at six weeks, as shown in Figure 9B. Although expression is seen at six weeks, the connexin-43 did not resemble coherent gap junctions, as shown in a piece of healthy myocardium (figure 10A).

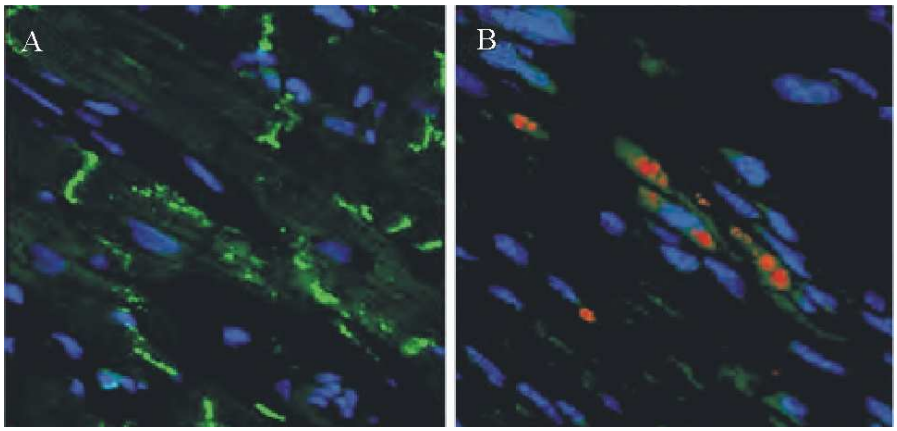

Figure 10. Connexin-43 expression in healthy myocardium (**A**) and infarcted tissue at sixth week (**B**). Connexin-43 is shown in green, IFP label in orange, and cell nuclei in blue. Note that the iron-labeled cells express the cardiac specific gap junction protein, connexin-43 (B).

C. Late desmin and connexin-43 expression

Eight animals were euthanized three months after surgery. After sacrifice, antibodies against desmin and connexin-43 were applied to sections of infarcted tissue. Cells containing iron-fluorescent particles as detected by confocal microscopy were found in 7/8 of the hearts (figure 11) and were not noted in the control group. In general, the cells exhibited striations typical of skeletal and cardiac muscle. Three-dimensional analysis of the confocal images confirmed the presence of iron particles within the cell boundary. In addition, gap junctions were noted in the form of intercalated disks, as shown in figure 12.

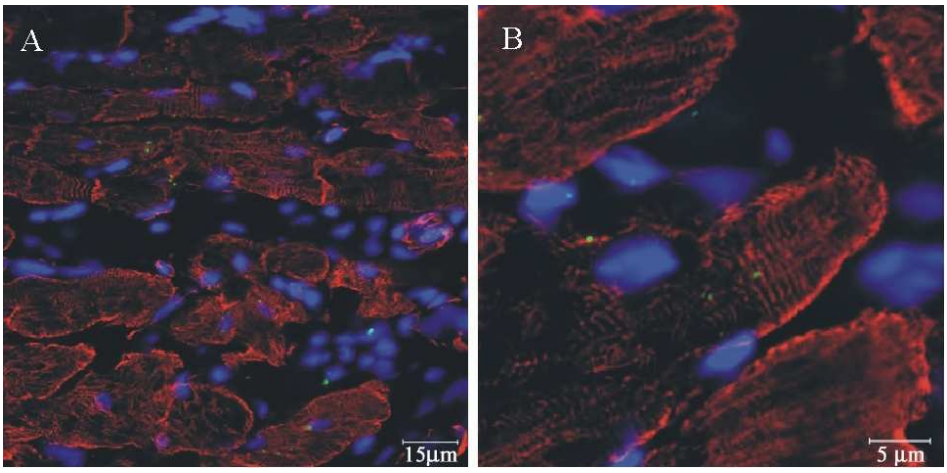

Figure 11. Desmin expression in infarcted tissue at third month. Desmin is shown in red, IFP label in green, and cell nuclei in blue (**A**). A high power view reveals striations similar to those found in muscle cells (**B**).

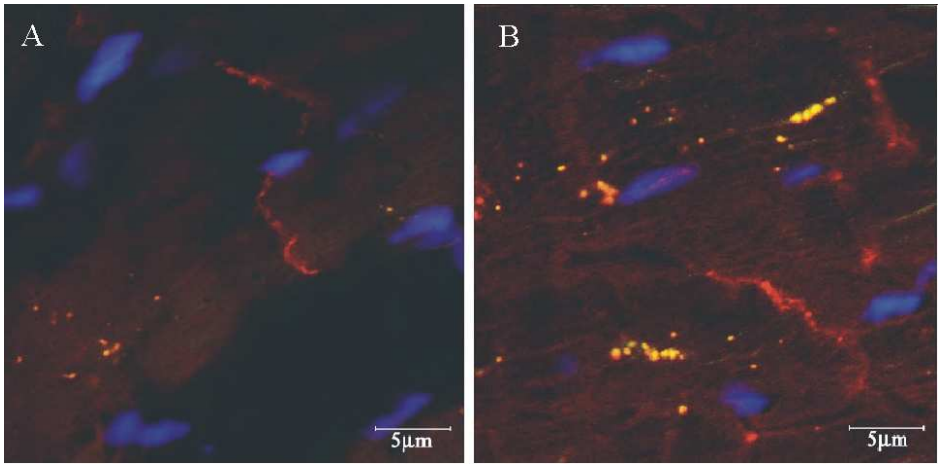

Figure 12. Connexin-43 expression by IFP-labeled cells three months after the procedure. Connexin-43 is shown in red, cell nuclei in blue, and the iron particles in yellow.

3. Cell distribution over time

While cell differentiation is of utmost importance when looking to repair damaged tissue through cell therapy, information pertaining to the length of time that the cells remain in the target organ is just as critical. Several groups have reported that stem cells injected within the core of an infarct do not persist for more than a couple of weeks[39].

Following cell injection, histology confirmed that the majority of cells were confined to the infarct region, although small numbers were seen basal to the infarct, near the coronary arteries. The numbers of cells increased from 745±230 per mm^2 at 24 hours to 2,190±302 at five days to 5,650±610 at six weeks (figure 13). Maximal engraftment of intravenously delivered MSCs was noted at six weeks. After six weeks, there was a dramatic fall off in IFP-labeled cell number within the infarct.

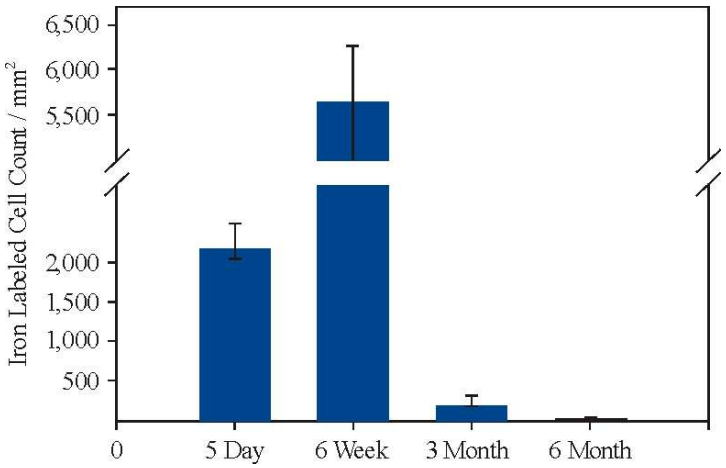

Figure 13. Quantification of cell engraftment over time. The maximum number of cells was seen in those animals euthanized six weeks after cell infusion. Although there were far fewer cells in the infarct zone at third and sixth month, those present phenotypically resemble cardiomyocytes.

4. Ejection fraction analysis

Results of the ejection fraction analysis are shown in figure 14 for 12 animals, seven treated and five controls, out to sixth month. While none of the results are statistically significant, a few generalizations can be made. First, the decrease in ejection fraction of the treated animals was less than that of the controls. In addition, at third and sixth month, there was a trend for the treated animals to exhibit greater recovery of function than that of the control group.

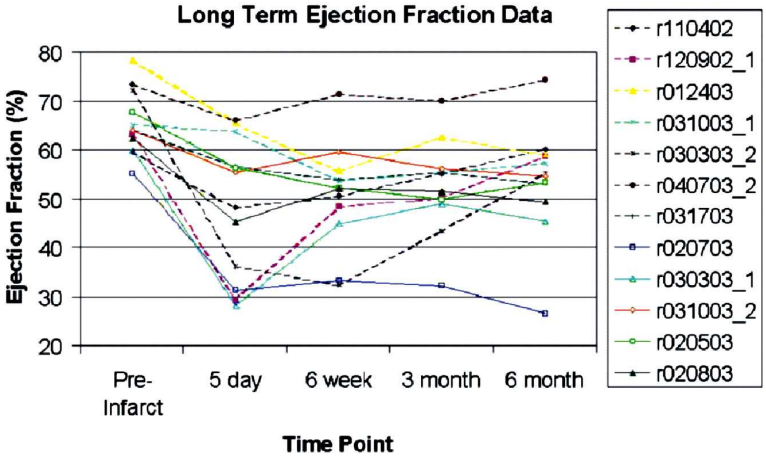

Figure 14. Ejection fraction data for eleven animals over six months. Dashed lines denote animals receiving MSCs, while control animals have solid lines.

5. Cell distribution to other organs

While cells preferentially homed to the injured myocardium, they were also found in large numbers throughout non-target organs. Systemically infused cells became lodged in the lungs immediately following infusion but tended to clear out after 48 hours in 4/4 animals examined. At this time point, significant numbers of cells were also found in the liver and spleen but were notably absent in the kidneys. Cells persisted in the liver and spleen out to sixth week, but were not noted at the third or sixth month endpoints.

IV. DISCUSSION

Recent evidence of the ability of stem cells to regenerate myocardium has been greeted with enthusiasm as well as a fair amount of skepticism. Thus far, few studies have demonstrated the capacity of various progenitor types to migrate regions of injury. Additionally, conventional stem cell studies largely rely on genetic labeling for stem cell identification in postmortem analyses. However, fundamental questions are extremely difficult to be answered using these ex vivo techniques. For example, to determine the bio-distribution of a graft, the entire organ must be sectioned and evaluated histologically. The present study demonstrates that iron-labeled, bone marrow-derived mesenchymal stem cells, when administered intravenously to rat model of myocardial infarction, home to sites of myocardial injury, which can be *in vivo* tracked by magnetic resonance imaging, have the capacity to differentiate into cells with cardiomyocyte phenotype expressing desmin and connexin-43 in spite of being labeled with iron microparticles, and contribute to functional improvement of infarcted heart.

Cell-based therapies to replace lost tissues in the damaged heart suggest a promising approach for the treatment of cardiac diseases. Different cell types have been assayed for their capacity to differentiate into cardiomyocytes. For instance, spontaneously contracting cardiomyocytes can easily be produced from embryonic stem cells *in vitro*[40]. These cells can even colonize the adult heart and differentiate into contractile tissues[39,41]. However, ES cellderived cardiomyocytes resemble cardiomyocytes of the primary heart tube[37], and the risk of uncontrolled proliferation of teratoma cells, as well as ethical reasons, is likely to reduce their wide use in therapies[42,43]. Adult hematopoietic stem cells, as well as stromal stem cells isolated from the bone marrow and endothelial progenitor cells, turn into cardiomyocytes under the appropriate culture conditions[44-47]. Furthermore, bone marrow (BM)-derived mesenchymal stem cells (MSCs) not only have high proliferative and self renewal capabilities, but can also secrete a broad spectrum of angiogenic cytokines and contain multipotent adult stem cells[48,49]. In addition, MSCs seem to lack immunogenecity, which may be a potential for allogeneic transplantation[50]. Therefore, allogeneic BM-derived MSCs used in this study would be the adequate cell type for stem cell transplantation because of their lack of immunogenicity as well as

relative ease of handling.

Homing, a process defined as migration of cells to target tissues, of transplanted stem cells to the injured sites is an essential step in engraftment and maintenance of regeneration. Adequate regulation of signaling between the bone marrow, the peripheral circulation and the infarcted myocardium is important in orchestrating the process of mobilization, homing, incorporation, survival, proliferation and differentiation of stem cells, that leads to myocardial regeneration. Although there are some proposed scenarios for homing of stem cells to areas of tissue injury; the basic concepts support the view that there are circulating stem cells that could originate from a common pool in bone marrow. This is further supported by findings that show that stem cells isolated from skeletal muscle retain hematopoietic activity and are itinerant cells derived from bone marrow[51-53]. Various signaling factors like as SDF-1, G-CSF, SCF, IL-8 and VEGF, known for their mobilizing and chemotactic abilities, are expressed after myocardial infarction in the setting of the pathophysiological healing process characterized with TNF-α, IL-8, IL-10, HIF-β, VEGF, and G-CSF although these factors and exact mechanisms for homing are poorly understood so far[54].

Actually, this study focused on tracking stem cell homing in vivo rather than looking for the mechanism of it because the ability to non-invasively track homing cells in vivo, following either local injection or intravenous administration, would provide insights into many basic and practical questions regarding these cell therapies. Hematopoietic progenitor cells have been labeled with membrane dyes and recovered from informative sites such as the marrow and spleen following intravenous admini- stration in murine models, but membrane dyes or other fluorescent labels require tissue sampling for detection, preventing real-time non-invasive tracking, except at very low resolution using new highly sensitive optical cameras[55,56]. Nuclear medicine techniques and PET scanning are under active development, but likely will never reach levels of sensitivity and resolution necessary for detection of small cell numbers or localization of these cells anatomically within organs[57]. Magnetic resonance imaging (MRI) has the potential to overcome these obstacles, by allowing serial non-invasive monitoring of administered cell populations, if cells can be made detectable via contrast agent loading[58]. The ability to localize or track specific cell populations in vivo via MRI has been pursued intensively over the past decade. A number of different contrast agents have been

developed, all predicated on loading cells with paramagnetic or superparamagnetic compounds. The first such experiments used fetal rat cells harvested from sheets of cortical tissue. Initial techniques to facilitate endogenous cellular uptake of superparamagnetic iron oxide particles included targeting to the transferrin receptor via monoclonal antibodies or liposomal coating and then membrane fusion, but neither resulted in efficient enough uptake for in vivo tracking, and there was significant cellular toxicity or impact on critical cellular characteristics[59,60]. Small superparamagnetic iron particles coated with dextran were taken up into cells via endocytosis and allowed dynamic tracking of loaded T cells to a site of inflammation in the rat testicle; this labeling enabled single cells to be detected *in vitro*[61,62]. Using the same approach, oligodendrocyte precursors have been labeled with small dextran superparamagnetic iron particles and localized after infusion into the brain of rats[63]. Recently, transferrin receptortargeted dextran-coated iron oxide nanoparticles were shown to have very efficient cellular uptake and were used to follow in vivo migration of labeled oligodendrocyte neural progenitor cells after injection into rat spinal cords; 50,000 labeled cells were injected at one site, and it is unclear what minimum number of cells localized in one area could be imaged using this contrast agent[64]. Weissleder and coworkers linked small dextran-coated fluorescent iron oxide particles to the 'tat' peptide from the human immunodeficiency virus. This translocation signal increased uptake of the particles up to 100-fold into lymphocytes and other hematopoietic cells, compared with particles without 'tat'[65]. Human $CD34^+$ cells labeled with these particles could be recovered from the marrow of immunodeficient mice following transplantation and detected via MRI in bones of these animals after removal of the bone from the whole mouse but not *in vivo* in real time following transplantation. Most recently, Bulte and coworkers have utilized a new contrast agent termed a magnetodendrimer, suspending iron oxide particles within a dendrimer matrix that is efficiently taken up into cells and optimized for favorable magnetic properties for imaging; 50,000 neural stem cells labeled with these particles could be detected *in vivo* following injection into the rat brain and used to track migration of the cells for up to 6 weeks[66]. Moreover, mixing ultra-small iron oxide particles with common lipofection agents has enabled efficient labeling of stem cells and in vivo tracking in the brain[67,68].

On the other hand, this study used fluorescent iron oxide polymer particles, which

offer several potential advantages for certain applications compared with previously described agents. Single cells have been detected in vitro after labeling with iron oxide, but this required very high resolutions[65,69]. The large particles should enable the presence of single cells to be detected at lower resolutions (200 μm) that can be achieved in vivo. These particles are much larger than other agents, with an average diameter of 0.9 to 1.0 μm. Hinds et al. showed that these larger particles created a much greater magnetic moment within individual cells, increasing the likelihood that in vivo imaging of single cells or very small numbers of cells will be possible[70]. These particles were taken up very rapidly and with high efficiency into all cell types analyzed to date, with no apparent toxicity or impact on bioactivity, despite dense loading of the cells with large iron particles. Moreover, the uptake of these particles did not appear to impact on the proliferative or differentiative potential of these cell populations. As mentioned in results, iron-labeled MSCs homed exactly to infarcted myocardium after intravenous administration as early as 5 days after injection, which could be in vivo tracked with MRI even though cells were found at other extracardiac tissues like as lung spleen. Moreover, these results compare favorably with a report published by Ciulla, who found that bone marrow mononuclear cells home to myocardial injury after a myocardial freeze-thaw injury[71]. However, the different method of creating myocardial damage coupled with the fact that cells were infused seven days post-injury make direct comparison with our results difficult. While the Ciulla group only examined one time point, cells were found in the spleen in addition to the injured myocardium. Other groups performing similar experiments in swine models of myocardial infarction have reported negative results, highlighting the possibility that the mechanisms behind homing are species-specific[72]. Many chemokines and receptor ligands are likely involved in the attraction and retention of stem cells to sites of tissue damage. The tissue microenvironment of the heart has been shown to induce the differentiation of many different cell types into those of a differentiated myocyte phenotype. *In vitro* preparations have demonstrated that MSCs can be coaxed into forming beating myotubes when provided with the appropriate signals[73]. Indeed, it had been shown that when treated with 5-azacytidine, and transplanted directly into a myocardial scar, MSCs reduce scar area, limit left ventricular dilatation and increase angiogenesis[74]. Untreated MSCs were shown to have no significant effect. More recently,

MSCs genetically engineered to produce the Akt1 gene and transplanted into ischemic rat myocardium were shown to reduce myocardial inflammation in addition to completely restoring normal cardiac function[75]. By these tracking results including this study, it is proposed that the ability of MRI to noninvasively track the migration of stem cells over many time points will enable scientists to determine which cytokines are necessary for this process to occur.

Desmin is the major intermediate filament protein of skeletal and cardiac muscle. It serves to link Z-bands with the sarcolemma and the myonuclei of a cell. Connexin-43 is a cardiac specific membrane protein that forms intercellular channels clustered together at gap junctions. Such channels allow ions and messenger to pass from one cell to its neighbors. Cells in a tissue must be coordinated so that growth, differentiation, apoptosis, wound healing, and homeostatic control can be maintained. One mechanism for such control is through coupling of the cells within a tissue via gap junctions. In terms of embryonic development, it has been shown that from day 13 onward, connexin-43 can be detected immunohistochemically in myocardium[76]. In this study, data indicate that IFP-labeled cells within the infarct region co-expressed desmin and connexin-43 as early as 6 weeks after injection suggesting that injected MSCs can differentiated into cells with phenotype of cardiomyocytes. In addition to differentiation, maturation of these two structural proteins is noted at 3 months after injection, that is, formation of striation typical of muscle cell and coherent gap junction at 3 months after injection. The possibility of this staining being an artifact (donor cells overlapped by recipient cardiomyocytes) can be ruled out because positive co-staining could be observed on consecutive 5-mm sections. If overlapping was responsible for this expression, multiple dual positive staining would not have been observed. The majority of studies using bone marrow cells demonstrated cardiomyocyte differentiation in vivo, following transplantations in animals similar to this study. Transcriptional profiles such as Nkx2.5, GATA-4, or MEF2 will help understanding the necessary molecular regulation of cardiac differentiation pathways. Recently, a clonal subpopulation of stem cells from adult bone marrow developed features of cardiomyocytes, endothelial cells and smooth muscle cells after co-culture with cardiomyocytes, which was partly the result of fusion[77]. In the present study, we were unable to examine the question of fusion between donor and host cells. Characterization of donor-derived cells in longer-term engraftment studies

may shed light on these questions.

To determine whether these microscopic findings can give rise to functional competence, left ventricle ejection fractions were evaluated with MRI. There is a trend for the MSCs-treated animals to exhibit greater recovery of systolic function than that of the control injected with only IFP devoid of MSCs even though the MRI parameters are not statistically significant.

V. CONCLUSION

Noninvasive imaging using MRI is very useful for tracking systemically injected MSCs labeled with iron-fluorescence particles, proposing that the response to stem cell therapy can be *in vivo* monitored with this technique. Additionally, this study demonstrated that homed MSCs can seed damaged myocardium and seem to differentiate into cells with cardiomyocyte phenotype, which might be related to functional improvement of infarcted heart. While there is the room to be filled with much evidences and the need to expand the scope of investigations, these findings should have exciting clinical potential for unveiling the homing mechanisms of stem cells.

REFERENCES

1. Shamblott MJ, Axelman J, Wang S, Bugg EM, Littlefield JW, Donovan PJ, et al. Derivation of pluripotent stem cells from cultured human primordial germ cells. Proc Natl Acad Sci USA 1998;95:13726-13731.
2. Thomson JA, Itskovitz-Eldor J, Shapiro SS, Waknitz MA, Swiergiel JJ, Marshall VS, et al. Embryonic stem cell lines derived from human blastocysts. Science 1998;282:1145-1147.
3. Kuznetsov SA, Krebsbach PH, Satomura K, Kerr J, Riminucci M, Benayahu D, et al. Single-colony derived strains of human marrow stromal fibroblasts form bone after transplantation *in vivo*. J Bone Miner Res 1997;12:1335-1347.
4. Prockop DJ. Marrow stromal cells as stem cells for nonhematopoietic tissues. Science 1997;276:71-74.
5. Pereira RF, Halford KW, O'Hara MD, Leeper DB, Sokolov BP, Pollard MD, et al. Cultured adherent cells from marrow can serve as long-lasting precursor cells for bone, cartilage, and lung in irradiated mice. Proc Natl Acad Sci USA 1995; 92:4857-4861.
6. Caplan AI. Mesenchymal stem cells. J Orthop Res 1991;9:641-650.
7. Friedenstein AJ. Precursor cells of mechanocytes. Int Rev Cytol 1976;47:327-359.
8. Owen M, Friedenstein AJ. Stromal stem cells: marrow-derived osteogenic precursors. Ciba Found Symp 1998;136:42-60.
9. Orlic D, Kajstura J, Chimenti S, Limana F, Jakoniuk I, Quaini F, et al. Transplanted adult bone marrow cells repair myocardial infarcts in mice. Ann NY Acad Sci 2001;938:221-229.
10. Jankowski RJ, Deasy BM, Huard J. Muscle-derived stem cells. Gene Ther 2002;9: 642-647.
11. Kopen GC, Prockop DJ, Phinney DG. Marrow stromal cells migrate throughout forebrain and cerebellum, and they differentiate into astrocytes after injection into neonatal mouse brains. Proc Natl Acad Sci USA 1999;96:10711-10716.
12. Makino S, Fukuda K, Miyoshi S, Konishi F, Kodama H, Pan J, et al. Cardiomyocytes can be generated from marrow stromal cells *in vitro*. J Clin Invest 1999;

103:697-705.
13. Ferrari G, Cusella-De Angelis G, Coletta M, Paolucci E, Stornaiuolo A, Cossu G, et al. Muscle regeneration by bone marrow-derived myogenic progenitors. Science 1998;279:1528-1530.
14. Orlic D, Kajstura J, Chimenti S, Limana F, Jakoniuk I, Quaini F, et al. Mobilized bone marrow cells repair the infarcted heart, improving function and survival. Proc Natl Acad Sci USA 2001;98:10344-10349.
15. Pittenger MF, Mackay AM, Beck SC, Jaiswal RK, Douglas R, Mosca JD, et al. Multilineage potential of adult human mesenchymal stem cells. Science 1999;284: 143-147.
16. Young HE, Mancini ML, Wright RP, Smith JC, Black AC Jr, Reagan CR, et al. Mesenchymal stem cells reside within the connective tissues of many organs. Dev Dyn 1995;202:137-144.
17. Quarto R, Thomas D, Liang CT. Bone progenitor cell deficits and the age-associated decline in bone repair capacity. Calcif Tissue Int 1995;56:123-129.
18. Azizi SA, Stokes D, Augelli BJ, DiGirolamo C, Prockop, DJ. Engraftment and migration of human bone marrow stromal cells implanted in the brains of albino rats--similarities to astrocyte grafts. Proc Natl Acad Sci USA 1998;95:3908-3913.
19. Toma C, Pittenger MF, Cahill KS, Byrne BJ, Kessler PD. Human mesenchymal stem cells differentiate to a cardiomyocyte phenotype in the adult murine heart. Circulation 2002;105:3-8.
20. Charron D. Immunogenomics of hematopoietic stem cell transplantation. Transfus Clin Biol 2003;10:156-158.
21. Falkenburg JH, van de Corput L, Marijt EW, Willemze R. Minor histocompatibility antigens in human stem cell transplantation. Exp Hematol 2003;31:743-751.
22. Horwitz EM, Gordon PL, Koo WK, Marx JC, Neel MD, McNall RY, et al. Isolated allogeneic bone marrow-derived mesenchymal cells engraft and stimulate growth in children with osteogenesis imperfecta: Implications for cell therapy of bone. Proc Natl Acad Sci USA 2002;99:8932-8937.
23. Josting A, Reiser M, Rueffer U, Salzberger B, Diehl V, Engert A. Treatment of primary progressive Hodgkin's and aggressive non-Hodgkin's lymphoma: Is there a chance for cure? J Clin Oncol 2000;18:332-339.

24. Vesole DH, Crowley JJ, Catchatourian R, Stiff PJ, Johnson DB, Cromer J, et al. High-dose melphalan with autotransplantation for refractory multiple myeloma: results of a Southwest Oncology Group phase II trial. J Clin Oncol 1999;17:2173-2179.
25. Friedenstein AJ, Piatetzky S II, Petrakova KV. Osteogenesis in transplants of bone marrow cells. J Embryol Exp Morphol 1996;16:381-90.
26. Pittenger MF, Mbalaviele G, Black M, Mosca JD, Marshak DR. in Human Cell Culture (eds. Kohller, M.R. & Palsson, B.O.) 189-207 (Kluwer Academic Publishers, Great Britain, 2001).
27. Devine SM, Bartholomew AM, Mahmud N, Nelson M, Patil S, Hardy W, et al. Mesenchymal stem cells are capable of homing to the bone marrow of non-human primates following systemic infusion. Exp Hematol 2001;29:244-255.
28. Yeh TC, Zhang W, Ildstad ST, Ho C. Intracellular labeling of T-cells with super-paramagnetic contrast agents. Magn Reson Med 1993;30:617-625.
29. Modo M, Cash D, Mellodew K, Williams SC, Fraser SE, Meade TJ, et al. Tracking transplanted stem cell migration using bifunctional, contrast agent-enhanced, magnetic resonance imaging. Neuroimage 2002;17:803-811.
30. Hoehn M, Kustermann E, Blunk J, Wiedermann D, Trapp T, Wecker S, et al. Monitoring of implanted stem cell migration in vivo: A highly resolved in vivo magnetic resonance imaging investigation of experimental stroke in rat. Proc Natl Acad Sci USA 2002;99:16267-16272.
31. Lois C, Alvarez-Buylla A. Long-distance neuronal migration in the adult mammalian brain. Science 1994;264:1145-1148.
32. Magavi SS, Leavitt BR, Macklis JD. Induction of neurogenesis in the neocortex of adult mice. Nature 2000;405:951-955.
33. Veizovic T, Beech JS, Stroemer RP, Watson WP, Hodges H. Resolution of stroke deficits following contralateral grafts of conditionally immortal neuroepithelial stem cells. Stroke 2001;32:1012-1019.
34. Bulte JW, Douglas T, Witwer B, Zhang SC, Strable E, Lewis BK, et al. Magnetodendrimers allow endosomal magnetic labeling and *in vivo* tracking of stem cells. Nat Biotechnol 2001;19:1141-1147.
35. Hinds KA, Hill JM, Shapiro EM, Laukkanen MO, Silva AC, Combs CA, et al.

Highly efficient endosomal labeling of progenitor and stem cells with large magnetic particles allows magnetic resonance imaging of single cells. Blood 2003;102:867-872.

36. Kraitchman DL, Heldman AW, Atalar E, Amado LC, Martin BJ, Pittenger MF, et al. *In Vivo* Magnetic Resonance Imaging of Mesenchymal Stem Cells in Myocardial Infarction. Circulation 2003;107:2290-2293.
37. Hill JM, Dick AJ, Raman VK, Thompson RB, Yu ZX, Hinds KA, et al. Serial Cardiac Magnetic Resonance Imaging (MRI) of Injected Mesenchymal Stem Cells. Circulation 2003;108:1009-1014.
38. Thomson JA, Itskovitz-Eldor J, Shapiro SS, Waknitz MA, Swiergiel JJ, Marshall VS, et al. Embryonic stem cell lines derived from human blastocysts. Science 1998;282:1145-1147.
39. Roell W, Lu ZJ, Bloch W, Siedner S, Tiemann K, Xia Y, et al. Cellular cardiomyoplasty improves survival after myocardial injury. Circulation 2002;105:2435-2441.
40. Mery A, Papadimou E, Zeineddine D, Menard C, Behfar A, Zingman LV, et al. Commitment of embryonic stem cells toward a cardiac lineage: molecular mechanisms and evidence for a promising therapeutic approach for heart failure. J Muscle Res Cell Motil 2003;24:269-274.
41. Behfar A, Zingman LV, Hodgson DM, Rauzier JM, Kane GC, Terzic A, et al. Stem cell differentiation requires a paracrine pathway in the heart. FASEB J 2002; 16:1558-1566.
42. Fijnvandraat AC, van Ginneken AC, Schumacher CA, Boheler KR, Lekanne Deprez RH, Christoffels VM, et al. Cardiomyocytes purified from differentiated embryonic stem cells exhibit characteristics of early chamber myocardium. J Mol Cell Cardiol 2003;35:1461-1472.
43. Pera MF, Filipczyk AA, Hawes SM, Laslett AL. Isolation, characterization, and differentiation of human embryonic stem cells. Methods Enzymol 2003;365:429-446.
44. Alison MR, Poulsom R, Forbes S, Wright NA. An introduction to stem cells. J Pathol 2002;197:419-423.
45. Fukuda K. Development of regenerative cardiomyocytes from mesenchymal stem cells for cardiovascular tissue engineering. Artif Organs 2001;25:187-193.
46. Makino S, Fukuda K, Miyoshi S, Konishi F, Kodama H, Pan J, et al. Cardio-

myocytes can be generated from marrow stromal cells *in vitro*. J Clin Invest 1999; 103:697-705.

47. Orlic D, Kajstura J, Chimenti S, Jakoniuk I, Anderson SM, Li B, et al. Bone marrow cells regenerate infarcted myocardium. Nature 2001;410:701705.
48. Badorff C, Brandes RP, Popp R, Rupp S, Urbich C, Aicher A, et al. Transdifferentiation of blood-derived human adult endothelial progenitor cells into functionally active cardiomyocytes. Circulation 2003;107:1024-1032.
49. Carlo-Stella C, Mangoni L, Rizzoli V. Biology and clinical applications of long-term bone marrow cultures. Int J Artif Organs 1993;16(Suppl 5):76-79.
50. Di Nicola M, Carlo-Stella C, Magni M, Milanesi M, Longoni PD, Matteucci P, Grisanti S, Gianni AM. Human bone marrow stromal cells suppress T-lymphocyte proliferation induced by cellular or nonspecific mitogenic stimuli. Blood 2002; 99: 38383843.
51. Issarachai S, Priestley GV, Nakamoto B, Papayannopoulou T. Cells with hemopoietic potential residing in muscle are itinerant bone marrowderived cells. Exp Hematol 2002;30:366373.
52. Kawada H, Ogawa M. Bone marrow origin of hematopoietic progenitors and stem cells in murine muscle. Blood 2001;98:20082013.
53. McKinney-Freeman SL, Jackson KA, Camargo FD, Ferrari G, Mavilio F, Goodell MA. Muscle-derived hematopoietic stem cells are hematopoietic in origin. Proc Natl Acad Sci USA 2002;99:13411346.
54. Vandervelde S, van Luyn MJ, Tio RA, Harmsen MC. Signaling factors in stem cell-mediated repair of infarcted myocardium. J Mol Cell Cardiol 2005;39:363-376.
55. Lanzkron SM, Collector MI, Sharkis SJ. Hematopoietic stem cell tracking in vivo: A comparison of short-term and long-term repopulating cells. Blood 1999;93:1916-1921.
56. Hardy J, Edinger M, Bachmann MH, Negrin RS, Fathman CG, Contag CH. Bioluminescence imaging of lymphocyte trafficking *in vivo*. Exp Hematol 2001;29: 1353-1360.
57. Adonai N, Nguyen KN, Walsh J, Iyer M, Toyokuni T, Phelps ME, et al. *Ex vivo* cell labeling with 64Cu-pyruvaldehyde- bis(N4-methylthiosemicarbazone) for imaging cell trafficking in mice with positron-emission tomography. Proc Natl Acad Sci USA 2002;99:3030-3035.

58. Allport JR, Weissleder R. *In vivo* imaging of gene and cell therapies. Exp Hematol. 2001;29:1237-1246.
59. Bulte JW, Hoekstra Y, Kamman RL, Magin RL, Webb AG, Briggs RW, et al. Specific MR imaging of human lymphocytes by monoclonal antibody-guided dextran-magnetite particles. Magn Reson Med 1992;25:148-157.
60. Bulte JW, Ma LD, Magin RL, Kamman RL, Hulstaert CE, Go KG, et al. Selective MR imaging of labeled human peripheral blood mononuclear cells by liposome mediated incorporation of dextran-magnetite particles. Magn Reson Med 1993; 29:32-37.
61. Yeh TC, Zhang W, Ildstad ST, Ho C. Intracellular labeling of T-cells with superparamagnetic contrast agents. Magn Reson Med 1993;30:617-625.
62. Yeh TC, Zhang W, Ildstad ST, Ho C. *In vivo* dynamic MRI tracking of rat T-cells labeled with superparamagnetic iron-oxide particles. Magn Reson Med 1995; 33:200-208.
63. Franklin RJ, Blaschuk KL, Bearchell MC, Prestoz LL, Setzu A, Brindle KM, et al. Magnetic resonance imaging of transplanted oligodendrocyte precursors in the rat brain. Neuroreport 1999;10:3961-3965.
64. Bulte JW, Zhang S, van Gelderen P, Herynek V, Jordan EK, Duncan ID, et al. Neurotransplantation of magnetically labeled oligodendrocyte progenitors: Magnetic resonance tracking of cell migration and myelination. Proc Natl Acad Sci USA 1999;96:15256-15261.
65. Lewin M, Carlesso N, Tung CH, Tang XW, Cory D, Scadden DT, et al. Tat peptidederivatized magnetic nanoparticles allow in vivo tracking and recovery of progenitor cells. Nat Biotechnol 2000;18:410-414.
66. Bulte JW, Douglas T, Witwer B, Zhang SC, Strable E, Lewis BK, et al. Magnetodendrimers allow endosomal magnetic labeling and in vivo tracking of stem cells. Nat Biotechnol 2001;19:1141-1147.
67. Hoehn M, Kustermann E, Blunk J, Wiedermann D, Trapp T, Wecker S, et al. Monitoring of implanted stem cell migration *in vivo*: A highly resolved in vivo magnetic resonance imaging investigation of experimental stroke in rat. Proc Natl Acad Sci USA 2002;99:16267-16272.
68. Frank JA, Zywicke H, Jordan EK, Mitchell J, Lewis BK, Miller B, Bryant LH

Jr, Bulte JW. et al. Magnetic intracellular labeling of mammalian cells by combining (FDA-approved) superparamagnetic iron oxide MR contrast agents and commonly used transfection agents. Acad Radiol 2002;9(Suppl 2):S484-S487.

69. Dodd SJ, Williams M, Suhan JP, Williams DS, Koretsky AP, Ho C. Detection of single mammalian cells by high-resolution magnetic resonance imaging. Biophys J 1999;76:103-109.
70. Hinds KA, Hill JM, Shapiro EM, Laukkanen MO, Silva AC, Combs CA, et al. Highly efficient endosomal labeling of progenitor and stem cells with large magnetic particles allows magnetic resonance imaging of single cells. Blood 2003;102: 867-872
71. Ciulla MM, Lazzari L, Pacchiana R, Esposito A, Bosari S, Ferrero S, et al. Homing of peripherally injected bone marrow cells in the rat after experimental myocardial injury. Haematologica 2003;88:614-621.
72. Chin BB, Nakamoto Y, Bulte JW, Pittenger MF, Wahl R, Kraitchman DL. ^{111}In oxine labelled mesenchymal stem cell SPECT after intravenous administration in myocardial infarction. Nucl Med Commun 2003;24:1149-1154.
73. Wakitani S, Saito T, Caplan AI. Myogenic cells derived from rat bone marrow mesenchymal stem cells exposed to 5-azacytidine. Muscle Nerve 1995;18:1417-1426.
74. Tomita S, Mickle DA, Weisel RD, Jia ZQ, Tumiati LC, Allidina Y, et al. Improved heart function with myogenesis and angiogenesis after autologous porcine bone marrow stromal cell transplantation. J Thorac Cardiovasc Surg 2002;123: 1132-1140.
75. Mangi AA, Noiseux N, Kong D, He H, Rezvani M, Ingwall JS, et al. Mesenchymal stem cells modified with Akt prevent remodeling and restore performance of infarcted hearts. Nat Med 2003;9:1195-1201.
76. van Kempen MJ, Fromaget C, Gros D, Moorman AF, Lamers WH. Spatial distribution of connexin43, the major cardiac gap junction protein, in the developing and adult rat heart. Circ Res 1991;68:1638-1651.
77. Yoon YS, Wecker A, Heyd L, Park JS, Tkebuchava T, Kusano K, et al. Clonally expanded novel multipotent stem cells from human bone marrow regenerate myocardium after myocardial infarction. J Clin Invest 2005;115:326-338.

ABSTRACT (IN KOREAN)

백서 경색 심근에서 전신적으로 주입된 철입자 표식 간엽줄기세포의 자기공명영상을 이용한 실시간 추적

<지도교수 조 승 연>

연세대학교 대학원 의과학과

홍 범 기

성체줄기세포를 이용한 세포 치료는 생체 내 이식의 양상이나 이식된 세포의 운명을 추적하기 어렵다는 제한을 갖고 있다. 최근 전신적으로 투여된 간엽줄기세포가 골수로 귀소하는 능력이 있음이 알려졌다. 줄기세포와 전구세포가 손상된 심근으로 귀소하는 사실은 심혈관 질환에 있어서 세포 치료에 대한 비침습적 접근을 가능하게 할 수 있는 하나의 중요한 기전이 된다. 초기에는 세포 조영 물질이 T 임파구의 이동을 추적하는데 사용되었으며, 그 후 신경학적인 응용으로 줄기세포를 추적하는데 이용되고 있다. 줄기세포의 이동이 설치류의 정상, 혹은 손상 받은 뇌조직에서 확인되고, gadolinium 조영제를 이용하여 이들을 추적하게 되었다. 최근에는, 철입자를 줄기세포나 전구세포의 표지자로 이용하는 방법이 개발되었는데, 이들은 이 세포들의 분화나 증식에 영향을 주지 않으며, 심근에 직접 주입한 후 세포의 이식을 추적하는데 유용한 방법임이 알려지게 되었다.

본 연구에서는, 철-형광입자로 표식된 간엽줄기세포를 심근 경색이 있는 쥐에게 전신적으로 주입한 후 이들을 자기공명영상을 이용한 비침습적 방법을 통해 생체 상태에서 추적할 수 있는지 알아보고, 이 세포들이 심근세포 특이 단백질을 발현하는지, 그리고 궁극적으로 손상된 심근의 기능적인 호전에 기여하는지 알아보고자 하였다.

August Copehagen Irish (ACI) 쥐의 좌관상동맥을 결찰하여 심근경색을 유발하고 다시 재관류시킨 후, 정맥 내로 동종의 철-형광입자로 표식된 간엽줄기세포를 주

입하거나(n=9), 혹은 단순히 철-형광입자만을 주입하고(n=9), 심장 자기공명영상 검사를 주입 후 5일, 6주, 3개월, 그리고 6개월째 시행하였다. 철-형광입자로 표식된 줄기세포는 심근세포의 표지 단백질인 desmin과 connexin-43를 이용한 면역조직화학 염색을 통해 동일초점 현미경으로 확인 하였다. 심장 조직에서 경색부와 비경색부에서 총 세포수를 확인하고, 이를 다시 철-형광입자로 표식된 세포의 수와 비교하였다.

철-형광입자로 표식된 간엽줄기세포는 경색 심근부위에서 주입 후 5일째부터 6개월째까지 확인이 되었는데 6주째 최고치를 보였다. 이 세포들은 특히 심근 손상이 있는 부위에 선택적으로 귀소하는 양상을 보여, 경색 심근부위와 정상 심근부위에서 총 세포수에 대한 철-형광입자로 표식된 세포의 비율이 의미있게 높았다(0.62 vs. 0.16, $p<0.01$). 6주째 이식된 세포는 근육원섬유 단백(desmin)과 간근결합 단백(connexin-43)을 발현하기 시작하였으며 3개월째 구조적 형태가 성숙되는 양상을 보였다. 좌심구혈률은, 비록 통계적인 의의는 보이지 않았지만, 간엽줄기세포를 주입하지 않은 군에 비해 세포를 주입한 군에서 더 호전되는 경향을 보였다.

이 연구를 통해 자기공명영상을 이용한 방법은 동종의 간엽줄기세포 이식의 귀소와 선택적인 이식 양상을 추적하는데 매우 유용하며, 이를 통해 이식된 줄기세포의 생체내 분화 과정을 추적할 수 있을 것으로 사료된다.

핵심 되는 말: 간엽줄기세포, 철-형광입자, 심근경색, 자기공명영상, 귀소, 분화, desmin, connexin-43